Journal of Medicinal Chemistry

Article

pubs.acs.org/jmc

Enhanced in Vitro Biological Activity of Synthetic 2-(2-Pyridyl) Ethyl Isothiocyanate Compared to Natural 4-(Methylsulfinyl) Butyl Isothiocyanate

Antonietta Melchini, Paul W. Needs, Richard F. Mithen, and Maria H. Traka*

Food & Health Programme, Institute of Food Research, Norwich Research Park, NR4 7UA United Kingdom

Supporting Information

ABSTRACT: Dietary isothiocyanates (ITC) derived from cruciferous vegetables have been shown to have numerous biological effects consistent with chemoprotective activity. In this study we synthesized a novel ITC, 2-(2-pyridyl) ethyl ITC (PY-ITC), and assessed its chemopreventive ability in comparison to sulforaphane (SF), the ITC derived from broccoli. PY-ITC suppressed cancerous cell growth and proliferation at lower concentrations than SF and was more potent at inducing p21 protein. Through the use of whole genome arrays we demonstrate that prostate cells exposed to PY-ITC or SF have similar biological response, albeit PY-ITC alters a greater number of genes, and to a greater extent. In the presence of a phosphatidylinositol-3-kinase (PI3K) inhibitor PY-ITC had a more pronounced effect on gene expression, emphasizing the important role of PI3K/AKT signaling in mediating the chemopreventive effects of ITCs. These results highlight the importance of the ITC side chain in bioactivity.

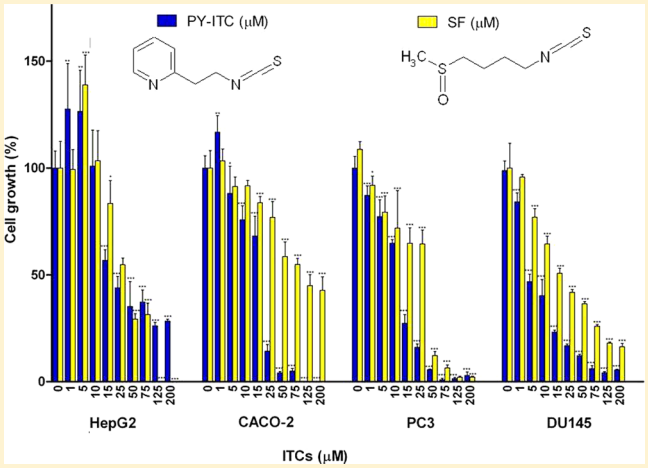

INTRODUCTION

Isothiocyanates (ITCs) are plant secondary metabolites derived from cruciferous vegetables. They have been well-studied for their pharmacokinetic properties and human health-promoting effects, including their potential to prevent chronic diseases such as cancer and cardiovascular disease, largely through the use of cell and animal models.[1] The ITC molecule consists of a core N═C═S moiety and a variable side chain, which accounts for the plethora of structures seen in cruciferous vegetables. By far the most well-studied ITC is 4-(methylsulfinyl) butyl ITC, commonly known as sulforaphane (SF), derived from broccoli (*Brassica oleracea* ssp. *italica*). The bioactivity of SF has been demonstrated in a variety of tissues, primarily through cell and animal models, and is attributed to multiple mechanisms of action. These include inhibition of cytochrome p450 (CYP) enzymes (phase 1), enhancement of phase 2 detoxification enzymes via nuclear factor (erythroid-derived) 2 (Nrf2) activation, induction of apoptosis and cell cycle arrest, inhibition of inflammation, and modulation of cell signaling pathways.[2] In particular, the phosphatidylinositol-3-kinase (PI3K)/akt signaling pathway, a major oncogenic pathway that is activated in many cancers, seems to play a crucial role in mediating the effects of SF in different cell types. In prostate tissue of men that received a diet rich in high-glucoraphanin broccoli over a year, changes related to PI3K signaling were prominent,[3] whereas in a mouse model of prostate cancer SF was only able to affect gene expression in prostate tissue that was perturbed in PI3K signaling.[4]

Much of the biological effects of ITCs are likely to be mediated by protein binding and subsequent protein modification, which has been demonstrated for a number of ITCs (Table S1 in Supporting Information).[5,6] Indeed, Nrf2-induction of detoxification enzymes by SF is achieved by binding of SF to sulfhydryl groups of Kelch-like ECH-associated protein 1 (Keap1), a protein associated with Nrf2.[7−10] Similarly, direct binding and modification of critical cysteine residues of α-/β-tubulin by ITCs interfered with their polymerization as dimers into microtubules and subsequently caused cell growth arrest.[11−14] The anti-inflammatory properties exerted by ITCs have also been linked with their ability to covalently bind multiple cysteine residues of recognition membrane receptors (Toll-like receptors, TLR), which blocks downstream NF-kb activation in mouse macrophages.[15] Binding is not limited only to cysteine residues as SF has been shown to bind to the N-terminal proline residue of the macrophage migration inhibitory factor (MIF), a pro-inflammatory cytokine, to suppress inflammation,[16−18] and to the N-terminal amino acids of key oncogenic molecules such as transforming growth factor beta (TGF-β) and insulin.[3]

Different ITCs, varying only in the nature of their side chain, exhibit different potency in mediating their biological effects

Received: July 2, 2012
Published: September 24, 2012

(Table S1 in Supporting Information). The nature of the side chain of ITCs can influence not only their lipophilicity, which will affect bioavailability, but also the reactivity of the N═C═S moiety that is also important for protein binding.[19,20] For example, phenethyl- and benzyl ITCs, containing an aromatic ring, are more potent in binding and modifying α-tubulin than sulforaphane, containing an aliphatic side chain.[13] Novel ITCs have been synthesized to contain modifications in the side chain using primarily untargeted approaches, which resulted in identifying some that were more or less potent in inhibiting NF-kb and inducing antioxidant response element (ARE)-dependent gene expression than naturally occurring ITCs.[21,22] Similarly, novel SF analogues were found to be at best equally potent with SF in inducing phase 2 enzymes and reduced mammary tumor formation in rats.[23]

In this study, we synthesized a novel ITC with a 2-(2-pyridyl) ethyl side chain but intact N═C═S moiety (2-(2-pyridyl) ethyl ITC, PY-ITC) (Figure 1) that is likely to react more readily with

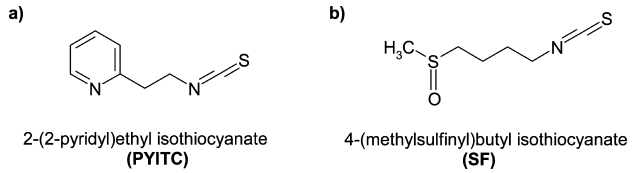

Figure 1. Molecular structures of the 2-(2-pyridyl) ethyl isothiocyanate (PY-ITC) (a) and the 4-(methylsulfinyl) butyl isothiocyanate (sulforaphane, SF) (b).

proteins and nucleophiles due to the possibility of intramolecular or general base catalysis and hypothesized that it will have stronger biological activity (Scheme 1). We first confirmed that

Scheme 1. Putative Mechanisms by which PY-ITC Might Enhance Its Substitution Rate: Intramolecular Nucleophilic Catalysis (a) and Intramolecular General Base Catalysis (b)

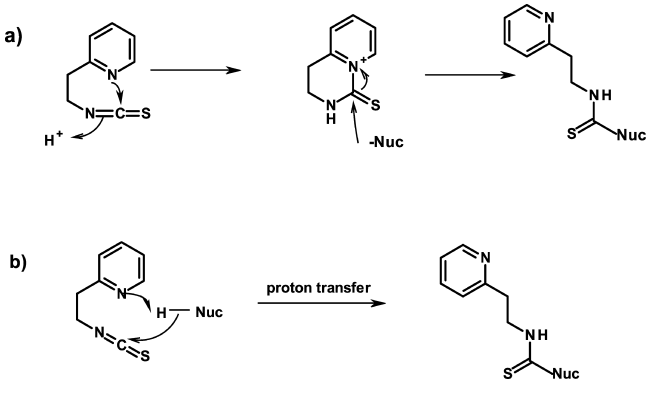

the synthetic PY-ITC binds more readily to biologically relevant proteins such as insulin than the naturally occurring SF and subsequently compared their bioactivity toward prostate cancer cells. We additionally assessed the role that the PI3K/akt signaling pathway plays in mediating the biological effects of these ITCs.

RESULTS

Synthesis of PY-ITC. PY-ITC was synthesized on the basis of a method for synthesis of thioureas as bronchodilators.[24] We treated 2-(2-aminoethyl)-pyridine with 1,1′-thiocarbonyldiimidazole and triethylamine (Scheme 2), to give 2-(2-pyridyl) ethyl

Scheme 2. PY-ITC Synthesis

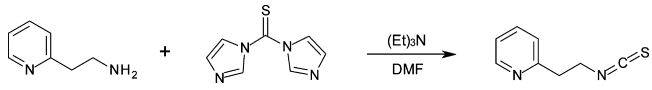

isothiocyanate (PY-ITC), which was purified by silica chromatography and distillation. The product was characterized and its purity confirmed by ^{1}H NMR, HPLC-ESI-MS, and HPLC-UV.

Binding Activity of PY-ITC and SF with Biorelevant Proteins. By analyzing in reverse phase HPLC the reaction mixtures of insulin and ITCs, we observed unreacted insulin, together with products with m/z values consistent with adducts of insulin containing either one or two additions of the ITC compounds (SF, PY-ITC) (Figure 2) (Figure S1 in Supporting Information). The relative ratios of the product to insulin peak areas indicated that the reaction with PY-ITC had progressed further than the reaction with SF. Thus, the reaction of PY-ITC with insulin was in turn quicker than the reaction with SF. The extinction coefficients of insulin and adducts are expected to be virtually identical, as none of the ITCs used, nor the expected thiourea adducts, absorb at 280 nm.

Rate of Reaction of PY-ITC and SF with Biorelevant Proteins. We have previously demonstrated that SF reacts selectively with the N-terminal amino groups of the A and B chains of insulin.[3] To assess the PY-ITC binding rate we used two pentapeptides, termed PPA and PPB, which had the amino acid sequence of the A and B N-terminuses of insulin, respectively. The reaction was assumed to proceed via a simple bimolecular rate determining step, and thus to conform to second-order kinetics. Furthermore, as the concentration of ITC used far exceeded that of the peptide, it was assumed that pseudo-first-order kinetics would be followed, and that a plot of the ln value of the peptide concentration against time should thus be linear. As the plot of the SIM peak area of both PPA and PPB against concentration was linear over the observed region (Figure 3), rate constants were determined from the slopes of a plot of decreasing ln(SIM peak area of PPA/B) against time. The rate of reactivity of SF with PPA and PPB was 1.4 and 1.7 $k_1/10^{-5}$ s^{-1}, respectively. Higher rates were observed for PY-ITC, 2.1 $k_1/10^{-5}$ s^{-1} (PPA) and 3.1 $k_1/10^{-5}$ s^{-1} (PPB). Each ITC reacted more quickly with the B chain pentapeptide than the A chain pentapeptide. As expected, only monosubstitution of either peptide was observed. The kinetic data obtained are listed in Table S2 in Supporting Information.

Effects of PY-ITC and SF on Cell Growth and Proliferation. We carried out a comparative study to evaluate the effects of PY-ITC and SF on cancer cell growth by using four human cancer cell lines from different origins (liver, HepG2; colon, Caco-2; prostate, PC3 and DU145). Results obtained from the WST-1 assay showed a dose-dependent decrease in cancer cell viability after treatment for 24 h with either ITC (Figure 4). PY-ITC was more effective compared to SF in reducing cell viability, and this effect was particularly prominent in prostate cancer cells (Table 1). Next, we assessed cell proliferation by measuring BrdU incorporation in PNT1A and PC3 cells. We found that concentrations of up to 50 μM of both PY-ITC and SF did not affect proliferation of normal PNT1A cells, while proliferation of PC3 cells was inhibited at concentrations close to physiologically relevant levels (Figure 5). PY-ITC inhibited the proliferation of PC3 cells by more than 80% at a concentration of 10 μM, whereas 25 μM was necessary

dx.doi.org/10.1021/jm300929v | J. Med. Chem. 2012, 55, 9682−9692

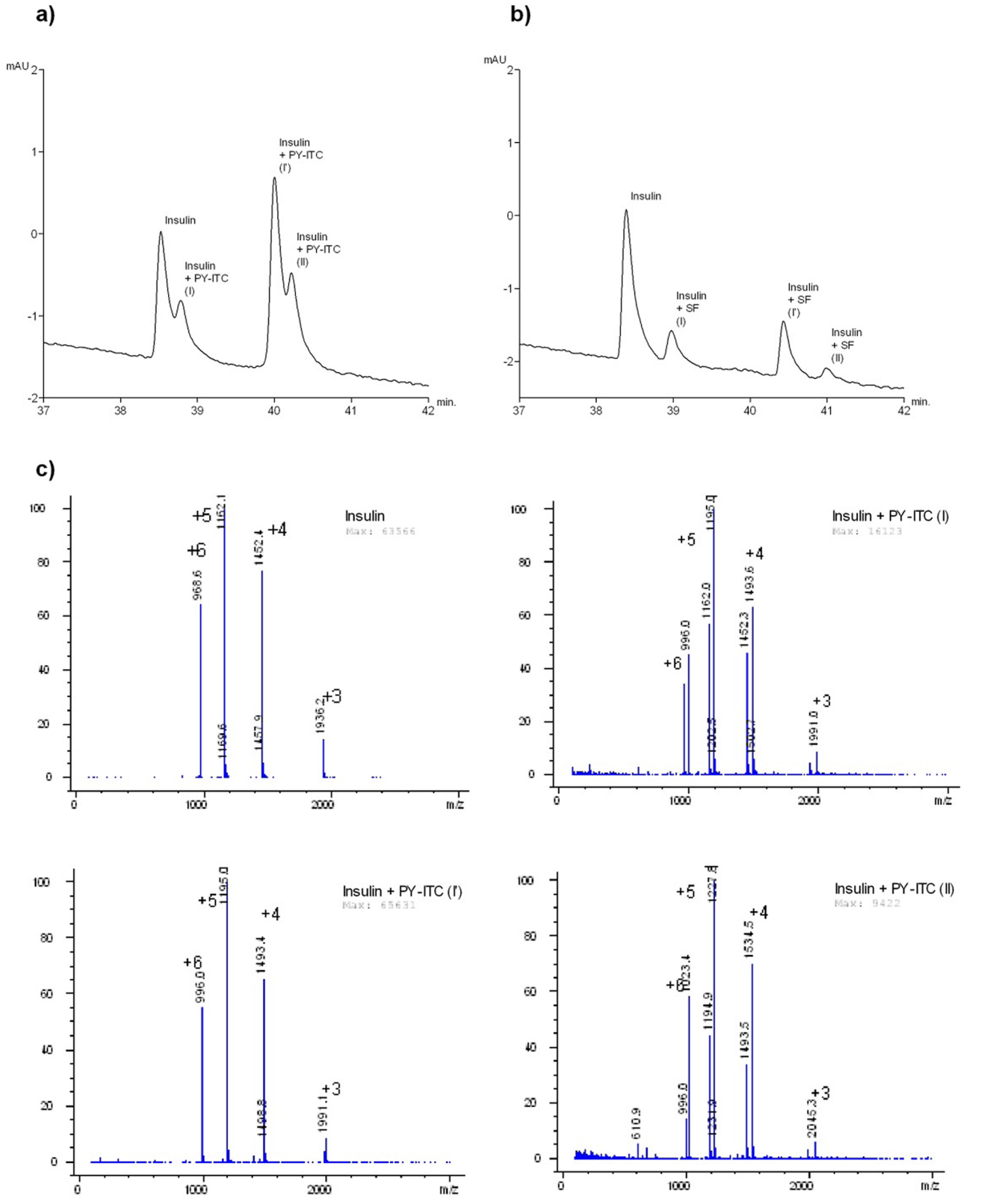

Figure 2. Reverse phase HPLC of insulin and ITC mixtures incubated for 6 h (280 nm detection). (a) Mixture of insulin and PY-ITC. (b) Mixture of insulin and SF. In each case, residual insulin, two monosubstituted adducts, and a disubstituted adduct were observed. The adducts were identified by their ESI-MS spectra. (c) MS spectra of the insulin-PY-ITC conjugates. See Figure S1 (Supporting Information) for MS spectra of the insulin-SF conjugates.

to observe a similar reduction with SF. The proliferative IC_{50} values clearly showed that PY-ITC has a higher selectivity in inhibiting cancerous cell proliferation than noncancerous.

Modulation of p21 Protein Expression by PY-ITC and SF. We next evaluated the biological activity of PY-ITC in comparison to SF by measuring protein expression of the cyclin-

dx.doi.org/10.1021/jm300929v | J. Med. Chem. 2012, 55, 9682−9692

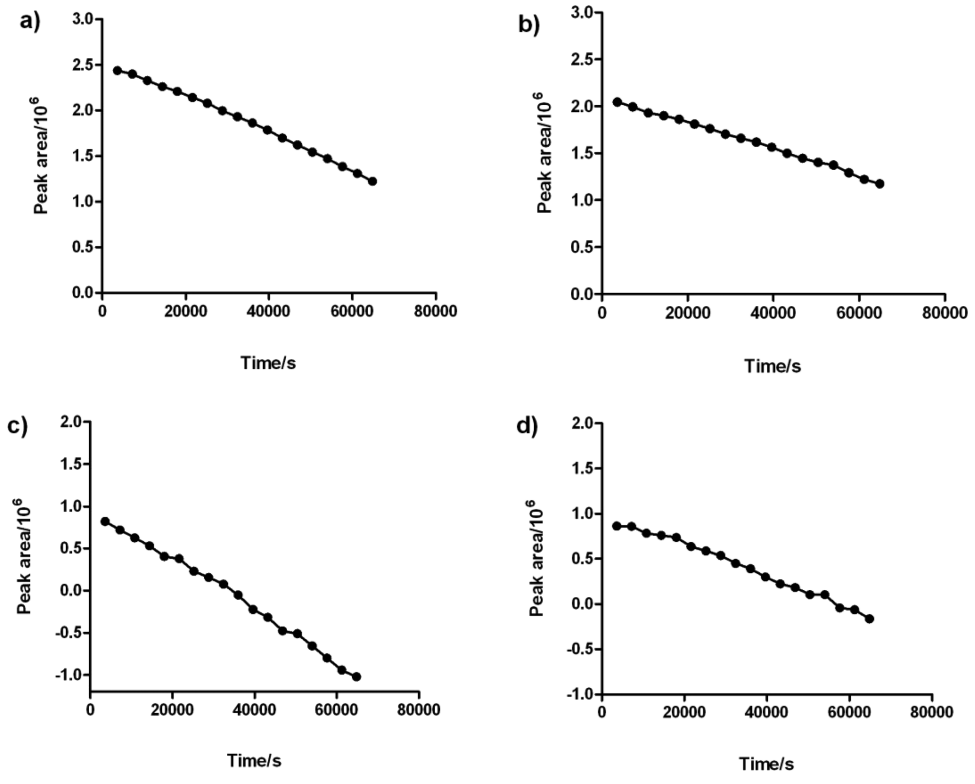

Figure 3. Kinetics of the reaction of PY-ITC with pentapeptides PPA (a) and PPB (b), and SF with PPA (c) and PPB (d). Selective ion monitoring (SIM) of the $[M + H]^+$ ion of PPA or PPB, over time, was used to determine the rates of reaction of the pentapeptides. Plots of $\log_e$(peptide peak area) against time are shown. The linear relationship is consistent with pseudo-first-order kinetics; pseudo k_1 values were calculated from the slopes of the plots.

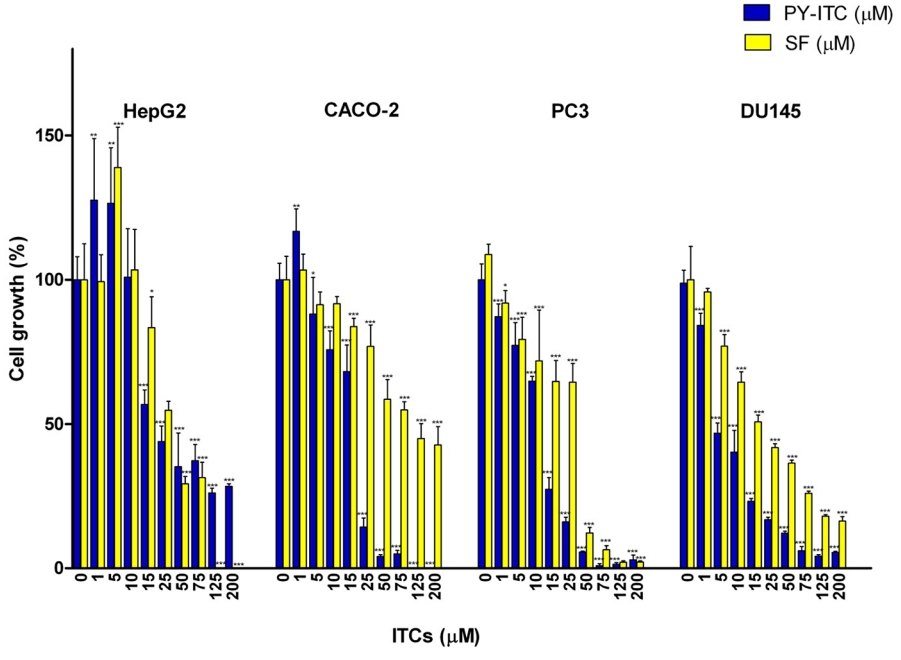

Figure 4. Effects of PY-ITC and SF treatment for 24 h on the viability of human cancer cell lines from different origins (liver, HepG2; colon, Caco-2; prostate, PC3 and DU145) as measured by the WST-1 assay. * $p < 0.05$, ** $p < 0.01$, *** $p < 0.001$ (significant differences between untreated and treated cells by 1-way ANOVA followed by Dunnett's posthoc test).

dependent kinase (CDK) inhibitor 1A (p21), an important modulator of cell cycle progression that can be regulated by the PI3K pathway[25] and a previous target identified for ITCs.[26,27] We used the PI3K inhibitor, LY294002, to suppress phosphorylation of Akt that is constitutively activated in cancerous PC3 cells due the presence of a nonfunctional PTEN allele.[28] In noncancerous PNT1A cells Akt is phosphorylated only in the presence of serum in the media (data not shown). PY-ITC

dx.doi.org/10.1021/jm300929v | J. Med. Chem. 2012, 55, 9682−9692

Table 1. IC_{50} of PY-ITC and SF on Human Cancer Cells from Different Origins[a]

	IC_{50} (μM)			
	hepatic HepG2	colon Caco-2	prostate DU145	prostate PC3
PY-ITC	15.31 ± 3.047	15.15 ± 2.204	4.436 ± 2.148	12.81 ± 0.878
SF	24.89 ± 1.533	79.83 ± 7.61	13.80 ± 2.866	32.38 ± 5.305

[a]Values are mean ± SD.

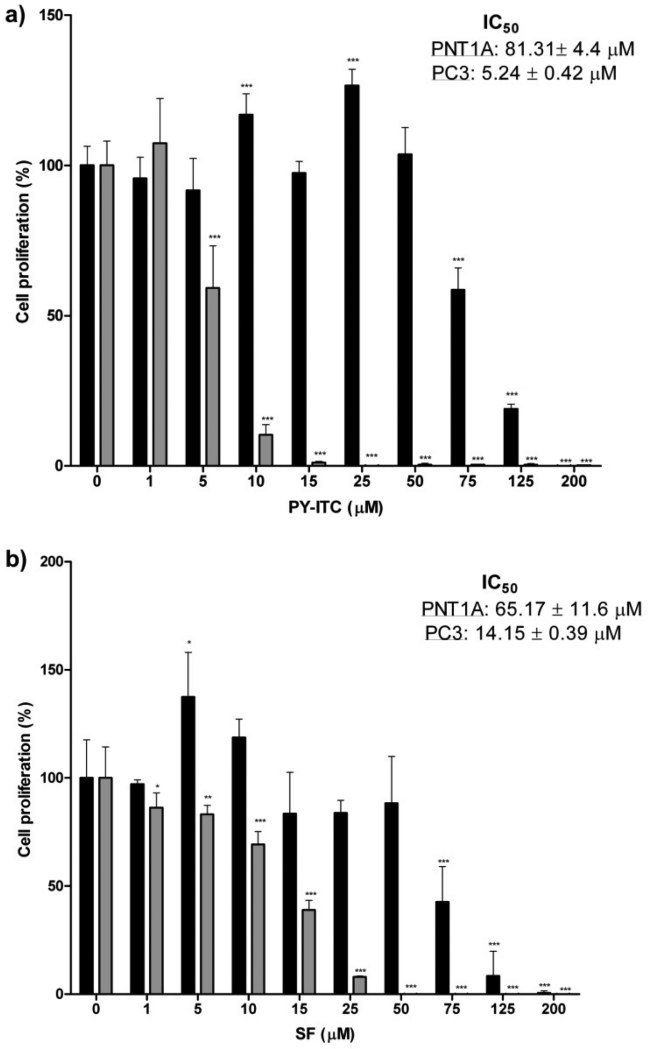

Figure 5. Effects of PY-ITC (a) and SF (b) treatment for 24 h on the proliferation of normal (PNT1A) and cancerous (PC3) prostate cells as measured by the BrdU assay. * $p < 0.05$, ** $p < 0.01$, *** $p < 0.001$ (significant differences between untreated and treated cells by 1-way ANOVA followed by Dunnett's posthoc test).

increased p21 protein levels by 3-fold in cancerous PC3 cells ($p \leq 0.05$) but had no effect in noncancerous PNT1A cells (Figure 6a). As expected, LY294002 treatment induced p21 protein expression in both cell lines, albeit not statistically significant. Interestingly, treatment with PY-ITC in the presence of the PI3K inhibitor increased p21 protein levels by approximately 8-fold in PC3 cells, which suggests there is an interaction between PY-ITC and PI3K inhibitor. Treatment with SF had similar effects on p21 protein expression, albeit at a lesser extent (Figure 6b).

Effects of PY-ITC and SF on Gene Expression in PNT1A and PC3 Prostate Cells. To assess additional effects of PY-ITC on prostate cells that would explain its antiproliferative properties we measured global gene expression using Affymetrix human exon arrays in PC3 and PNT1A cells in response to treatment with PY-ITC and compared it to SF. PY-ITC was found to be more potent in inducing gene changes than SF, and the effect was more prominent in the cancerous PC3 cells than the noncancerous PNT1A cells (Table 2). Indeed, PY-ITC induced 508 transcripts in PNT1A cells compared to 153 by SF, whereas in PC3 cells PY-ITC induced 2973 transcripts compared to 71 by SF ($p \leq 0.01$). Consistent with previous reports of the effect of ITCs on cells, SF and PY-ITC altered genes involved in apoptosis, mitogen-activated protein kinase (MAPK) signaling, and cytokine receptor signaling pathways in PNT1A cells (Table 3). In PC3 cells PY-ITC additionally changed significantly genes associated with cell cycle, amino acid metabolism, and growth factor signaling pathways (Table 4). Of the genes induced by the two ITCs, 238 genes were common between SF and PY-ITC in PNT1A cells and 159 genes in PC3 cells ($p \leq 0.05$) (Figure 7a,b). These common genes were associated with apoptosis, NOD- and Toll-like receptor signaling, and chemokine/cytokine signaling pathways (data not shown). Although these common genes changed in the same direction with both ITCs, PY-ITC was more potent than SF in inducing them by 26% and 46%, in PNT1A and PC3 cells, respectively (Figure 7c,d).

Role of the PI3K Pathway in ITC-Mediated Transcriptional Activity of PNT1A and PC3 Prostate Cells. To examine how the PI3K/Akt pathway can regulate gene expression in our cell system and further explore the interaction with ITCs, we also performed microarray analyses on PNT1A and PC3 cells treated with a highly specific PI3K inhibitor. LY294002 is inducing significant gene expression changes in both the benign PNT1A and cancerous PC3 cells, 3095 and 2270 genes, respectively. Consistent with perturbation of the pAkt signaling pathway these genes were associated with amino acid and phosphate metabolism and mTOR signaling pathway (Tables S3−S4 in Supporting Information).

To determine whether PY-ITC and SF have a PI3K inhibitor activity we compared their effect on gene expression. A high proportion of genes changed by SF and PY-ITC ($p \leq 0.05$) were also targets of the PI3K inhibitor (Figure 8), and the majority of these changed in the same direction albeit to a lesser extent (data not shown), which suggests that at least partly both ITCs are acting as a PI3K inhibitor. In both cell lines a higher proportion of genes changed by the PI3K inhibitor were also changed in a similar way by PY-ITC compared to SF. Indeed, 37.5% and 9.3% of the genes changed by the PI3K inhibitor also changed in a similar way by the PY-ITC treatment in PC3 and PNT1A cells, respectively (Figure 8c,d), whereas less than 3% also changed by SF (Figure 8a,b). These results suggest that both ITCs act at least partly as a PI3K inhibitor but also have additional functions that are specific to these ITCs.

In the presence of the PI3K inhibitor, both PY-ITC and SF had a more pronounced effect on gene expression than when the PI3K pathway was activated (Table 2). PY-ITC, in particular, induced more gene changes associated with metabolic and phosphatidylinositol signaling pathways than in the absence of

dx.doi.org/10.1021/jm300929v | J. Med. Chem. 2012, 55, 9682−9692

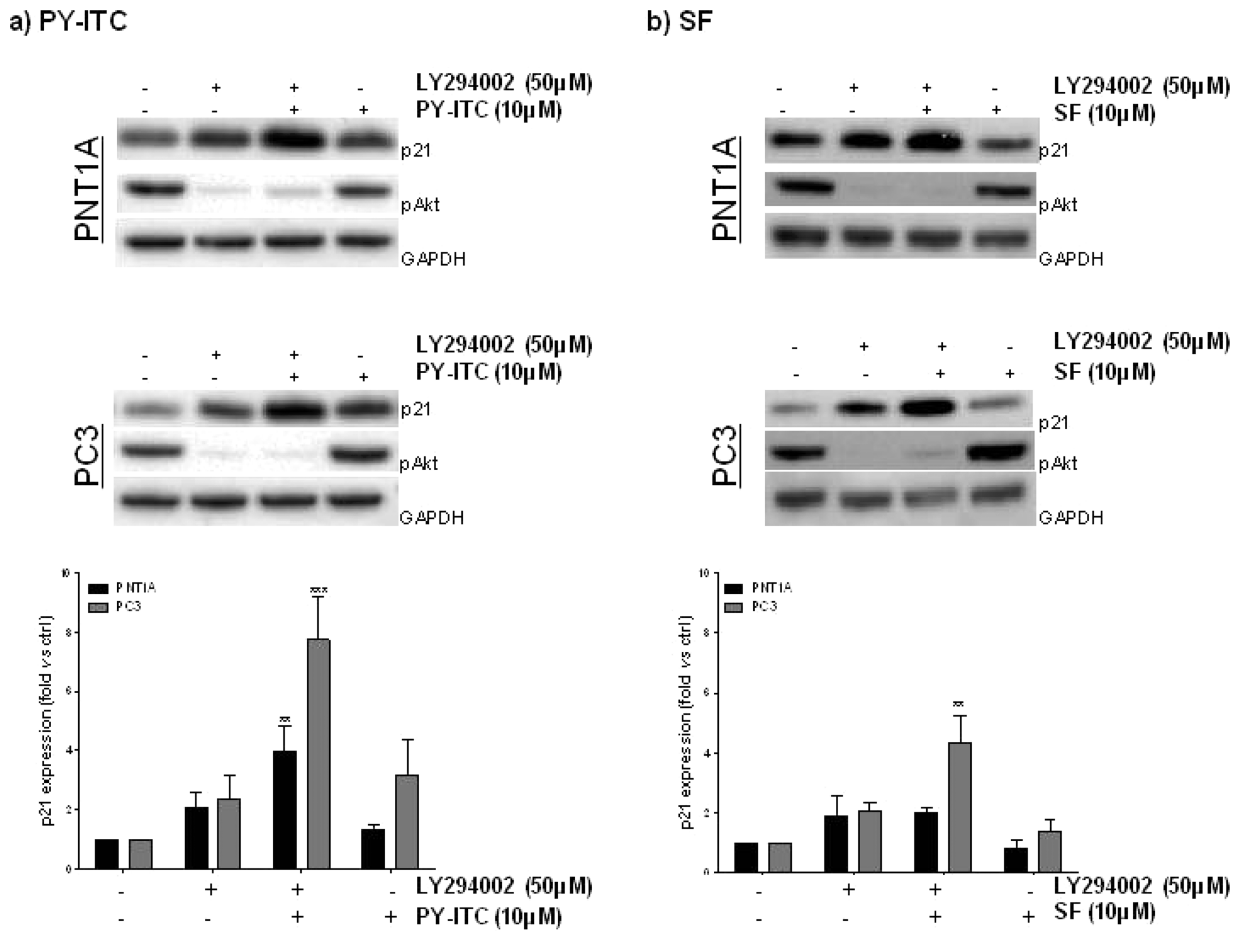

Figure 6. Western blot detection of p21 and pAkt protein levels in normal (PNT1A) and cancerous (PC3) prostate cells after 8 h treatment with PY-ITC and SF in the presence of the PI3K inhibitor. Quantitative analysis of protein levels was performed using Quantity One software. Data shown are mean ± SD of three replicate experiments. GAPDH was used to confirm equal protein loading. * $p < 0.05$, ** $p < 0.01$, *** $p < 0.001$ (significant differences between untreated and treated cells by 1-way ANOVA followed by Tukey's posthoc test).

Table 2. Changes in Transcript Expression in PNT1A and PC3 Cells by SF and PY-ITC in the Presence or Absence of the PI3K Inhibitor LY294002[a]

	$p \leq 0.05$	$p \leq 0.01$	$p \leq 0.001$
PNT1A Cells			
Co vs PY-ITC	961	508	247
Co vs SF	334	153	59
Co vs Inh	4387	3095	1976
Inh vs Inh + PY-ITC	3365	2111	1144
Inh vs Inh + SF	477	183	68
PC3 Cells			
Co vs PY-ITC	7790	2973	1350
Co vs SF	199	71	23
Co vs Inh	3533	2270	1318
Inh vs Inh + PY-ITC	4885	3414	2191
Inh vs Inh + SF	1233	523	169

[a]Cells were treated with vehicle DMSO (Co), 10 μM PY-ITC, or 10 μM SF for 8 h. To inhibit the PI3K pathway cells were also pretreated for 1 h with 50 μM PI3K inhibitor LY294002 (Inh).

the inhibitor (Tables 3and 4) (Tables S5 and S6 in Supporting Information), which suggests ITCs are interacting with the PI3K signaling pathway.

DISCUSSION AND CONCLUSIONS

Many studies with cell and animal models have now described the multiple biological activities of dietary isothiocyanates. An emerging underpinning theme to explain the complex activities of these compounds is their propensity to conjugate with proteins either through sulfhydryl or amino groups. This activity may be partly facilitated by the intramolecular catalysis of the ITC side chain, which may explain some of the variation in bioactivity between naturally occurring ITCs. To explore this, we synthesized PY-ITC, an ITC compound with the 2-(2-pyridyl) ethyl side chain that might have enhanced reactivity with proteins through intramolecular or general base catalysis of the nucleophilic addition. The high polarity of the pyridyl group would confer relatively high solubility at neutral pH, and a pK_a close to physiological pH might allow intramolecular nucleophilic, or a general base catalysis of, addition to the isothiocyanate group. In addition, any nucleophilic catalysis would occur via a favorable six membered ring intermediate (Scheme 1). Proving this is not within the scope of this work and would involve undertaking a classical kinetic study, using isotopic labeling techniques; the relatively small rate enhancements we observed would also make this particularly challenging.

Initially, we showed that PY-ITC suppressed the growth and proliferation of various cancer cells at a lower concentration than the naturally occurring dietary ITC sulforaphane, and that this was associated with a greater induction of p21 (Figure 6). To

dx.doi.org/10.1021/jm300929v | J. Med. Chem. 2012, 55, 9682−9692

Table 3. Functional Analysis of Genes Changed by SF and PY-ITC in PNT1A Cells ($p \leq 0.01$)

term	count	*p*-value	fold enrichment
SF			
Cell Growth			
apoptosis	6	0.01	4.8
Signaling Pathways			
toll-like receptor signaling pathway	5	0.05	3.5
cytokine−cytokine receptor interaction	12	<0.01	3.3
MAPK signaling pathway	9	0.03	2.4
Other			
graft-versus-host disease	3	0.07	6.9
systemic lupus erythematosus	5	0.03	4.3
hematopoietic cell lineage	5	0.03	4.3
PY-ITC			
Cell Growth			
apoptosis	8	0.04	2.5
Signaling Pathways			
TGF-beta signaling pathway	7	0.10	2.2
cytokine−cytokine receptor interaction	16	0.05	1.7
MAPK signaling pathway	16	0.06	1.7
Other			
systemic lupus erythematosus	11	<0.01	3.6
glycine, serine, and threonine metabolism	5	0.08	3.1
glutathione metabolism	5	0.10	2.8
colorectal cancer	7	0.09	2.2
melanogenesis	8	0.07	2.2
axon guidance	9	0.09	1.9

Table 4. Functional Analysis of Genes Changed by SF and PY-ITC in PC3 Cells ($p \leq 0.01$)

term	count	*p*-value	fold enrichment
SF			
apoptosis	4	0.02	0.02
toll-like receptor signaling pathway	4	0.02	0.02
MAPK signaling pathway	5	0.07	0.07
PY-ITC			
Cell Growth			
DNA replication	18	<0.01	3.1
cell cycle	48	<0.01	2.6
apoptosis	27	<0.01	1.9
Signaling Pathways			
p53 signaling pathway	24	<0.01	2.1
ErbB signaling pathway	22	0.02	1.6
epithelial cell signaling in *Helicobacter pylori* infection	17	0.07	1.6
TGF-beta signaling pathway	21	0.05	1.5
Cancer-Related Pathways			
pancreatic cancer	26	<0.01	2.2
glioma	19	0.01	1.9
prostate cancer	28	<0.01	1.9
chronic myeloid leukemia	22	<0.01	1.9
nonsmall cell lung cancer	14	0.07	1.7
small cell lung cancer	22	0.03	1.6
colorectal cancer	21	0.05	1.5
Metabolism			
alanine and aspartate metabolism	9	0.07	2.0
lysine degradation	14	0.04	1.8
glycolysis/gluconeogenesis	16	0.05	1.6
pyrimidine metabolism	25	0.01	1.6
Other			
mismatch repair	10	0.01	2.6
homologous recombination	11	0.01	2.4
base excision repair	12	0.02	2.1
aminoacyl-tRNA biosynthesis	12	0.06	1.8
systemic lupus erythematosus	24	<0.01	1.8
nucleotide excision repair	13	0.05	1.8
ABC transporters	12	0.10	1.6
one carbon pool by folate	7	0.03	2.8

further investigate the enhanced bioactivity of PY-ITC we used prostate cells as a model to measure global gene expression changes in response to PY-ITC and compared it to SF. We found that PY-ITC was more potent in inducing gene changes than SF, but affected similar functional pathways, and the effect was more prominent in the cancerous PC3 prostate cells than the noncancerous PNT1A prostate cells (Table 2). As enhancement of the PI3K signaling pathway is a driver of malignant transformation in prostate,[29] we studied the interaction of PY-ITC with the PI3K signaling pathway. Pharmacological inhibition of this pathway has been considered a promising strategy in the intervention of prostate cancer.[30] We found that both ITCs and in particular PY-ITC have similar biological effects as a PI3K inhibitor, which would explain their antiproliferative and growth suppressive properties. In addition, PY-ITC, more so than SF, enhanced the effects of the PI3K inhibitor by inducing more genes associated with PI3K-signaling pathways. Consistent with this, PY-ITC synergistically enhanced the effect of the PI3K inhibitor on the induction of p21 protein. These results confirm that introducing slight modifications in the side chain of ITCs can translate to enhanced bioactivity and pave the way for a new class of compounds with improved anticancer effects.

To date, in contrast to many other natural products, isothiocyanates have not been extensively used as therapeutic agents themselves nor have they formed the basis of synthetic pharmaceutical agents. This is partly due to their complex biological activity with many potential molecular targets, and partly due to issues concerning delivery. Recently, SF has begun to be used in human studies to target early stages of prostate cancer, largely underpinned by substantial data from animal models. Currently there are three active clinical intervention trials in the U.S. aimed to assess the protective properties of SF delivering supplements in prostate cancer, as reported by ClinicalTrials.gov.[31−33] The complex etiology of prostate cancer may indeed make it a suitable target for compounds such as SF. Loss of the PTEN tumor suppressor and activation of PI3K/akt signaling is frequently associated with prostate cancer progression, and the enhanced activity of SF in tissue that has PTEN loss[4] may again suggest that SF could be an appropriate therapeutic agent. In the current study we have shown that exchanging the methylsulfinylbutyl side chain of SF with a 2-(2-pyridyl) ethyl side chain results in a faster interaction with proteins and an associated increase in biological activity concerned with suppression of proliferation of cancer cells and induction of gene expression. While we are not advocating PY-ITC itself as a therapeutic agent, this study is the first to rationally design an ITC to enhance activity. As with many potential therapeutic agents, delivery of synthetic and natural ITCs to target tissues is a major issue. Aside from the anticarcinogenic activity, ITCs have also been shown to have potent antimicrobial activity, such as suppression of *Helicobacter pylori* and urinary infections within mammals.[34−36] Although this area has been less

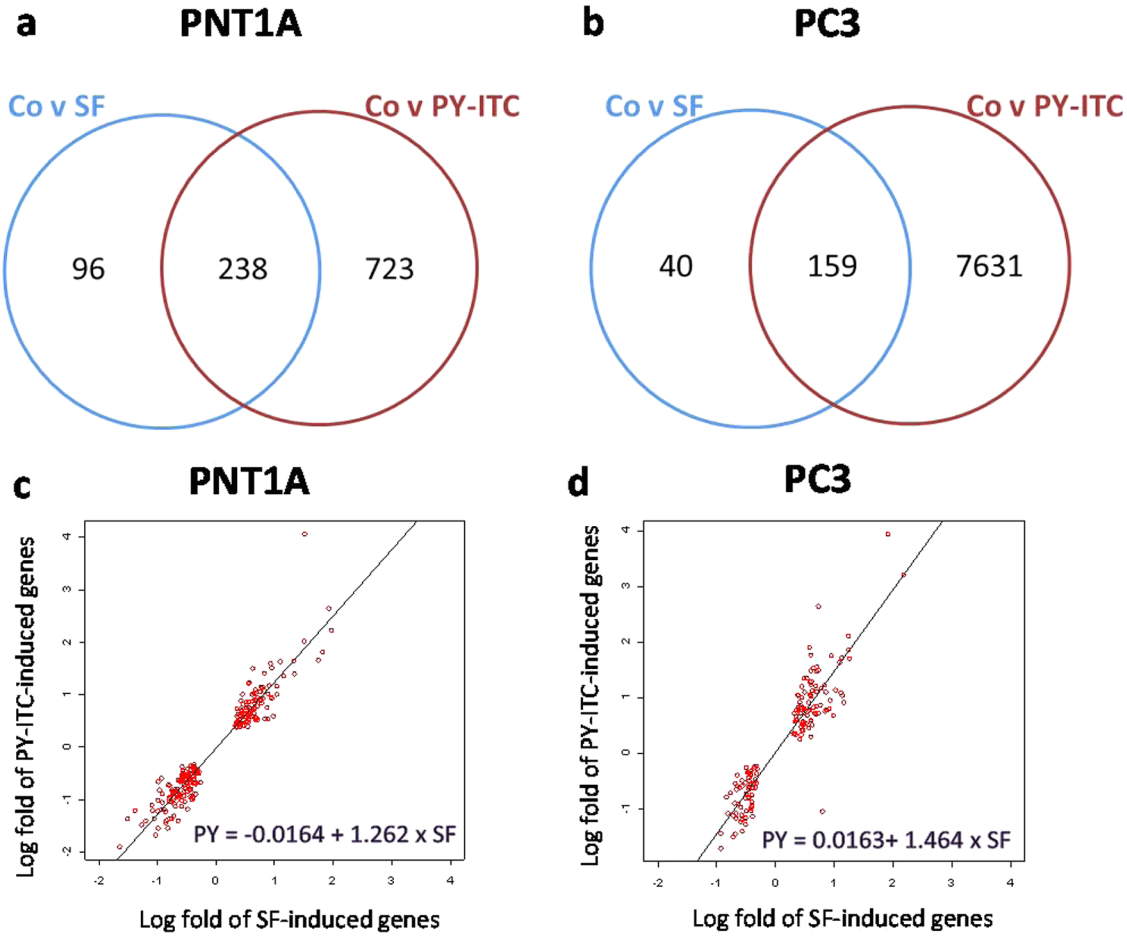

Figure 7. Transcripts common between SF and PY-ITC treatments in PNT1A cells (a) and PC3 cells (b). Magnitude of change in the common genes between SF and PY-ITC treatments in PNT1A (c) and PC3 cells (d).

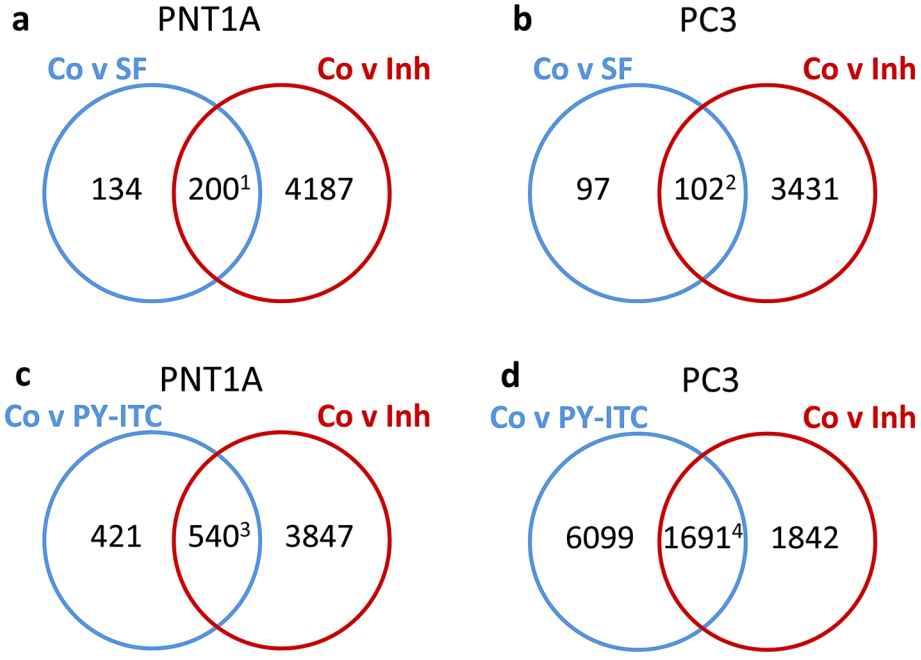

Figure 8. Transcripts common between SF (a, b) or PY-ITC (c, d) and PI3K inhibitor treatments in PNT1A cells (a, c) and PC3 cells (b, d). Superscript numbers indicate the following: (1) 2.6% of PI3kinh-induced genes are also changed by SF in the same direction. (2) 1.4% of PI3kinh-induced genes are also changed by SF in the same direction. (3) 9.3% of PI3kinh-induced genes are also changed by SF in the same direction. (4) 37.5% of PI3kinh-induced genes are also changed by SF in the same direction.

dx.doi.org/10.1021/jm300929v | J. Med. Chem. 2012, 55, 9682−9692

studied than cancer prevention it is conceivable that enhancing protein binding would also improve bioactivity of natural ITCs against microbial agents, but this remains to be tested.

EXPERIMENTAL SECTION

General. PY-ITC (purity ≥98%) was synthesized by Dr. Paul Needs at the Institute of Food Research, Norwich (U.K.). 2-(2-Aminoethyl)-pyridine, 1,1′-thiocarbonyldiimidazole, dimethylformamide (DMF), and triethylamine were obtained from Sigma Aldrich and used as supplied. NMR spectra were recorded on a Bruker Avance NMR spectrometer (Bruker BioSpin GmbH, Rheinstetten, Germany) equipped with a cryoprobe (TCI) and operating at 600 MHz for ^{1}H. IR spectra were recorded by attenuated total reflectance (ATR), using a BioRad FTS175C Fourier transform infrared spectrometer with HgCdTe detector and Specac GoldenGate single reflection diamond Horizontal ATR system. Medium performance liquid chromatography (MPLC) used 50 g prepacked silica cartridges (Isolute Flash Si, Biotage) and UV detection. HPLC-ESI-MS used a 5 mm C-18 Lunar column (250 mm × 4.4 mm) eluted at 1 mL/min at 30 °C with a 0.1% formic acid/0.1% formic acid in acetonitrile gradient. SF (purity >98%) (CAS 4478-93-7) was obtained from a commercial source (LKT Laboratories).

Synthesis of PY-ITC. PY-ITC was made by treatment of 2-(2-aminoethyl)pyridine with 1,1′-thiocarbonyldiimidazole and triethylamine as described by Berglund.[24] 1, 1,1′-Thiocarbonyldiimidazole (5 g, 1.2 equiv) was dissolved in dimethylformamide (DMF) (40 mL) at 50 °C. A solution of 2-(2-aminoethyl)pyridine (3.44 g, 28.1 mmol) and triethylamine (1 equiv) in DMF was then added dropwise. The mixture was stirred at room temperature for 2 h, diluted with water, and extracted with ethyl acetate (EtOAc). The combined organic phases were washed with water, dried ($MgSO_4$), and concentrated. The residue was purified by MPLC (silica gel, 1:1 EtOAc/hexane eluant) to give a yellow oil, which was further purified by bulb distillation under vacuum to give PY-ITC as a very pale yellow oil (1.40 g, 30%). PY-ITC purity was estimated by ^{1}H NMR, HPLC-ESI-MS, and HPLC-UV. ^{1}H NMR (400 MHz, chloroform-d) δ d 3.10 (t, J = 6.7 Hz, 2H), 3.90 (t, J = 6.7 Hz, 2H), 7.16 (m, 2H), 7.61 (td, J = 8.0, 1.8 Hz, 1H), 8.54 (bd d, J = 4.9 Hz, 1H). IR ν/cm^{-1} 2079, 2179. HPLC-ESIMS m/z 165 (M + H$^+$). Estimated purity by HPLC-UV analysis at 270 nm was >98%.

Detection of in Vitro Adducts between ITCs and Insulin. Reverse phase HPLC examination of insulin and ITC reaction mixtures, after 6 h in phosphate buffered saline (PBS) at 37 °C, revealed insulin-ITC adducts, which were quantified by their absorption at 280 nm. Peak assignments were made by ESI-MS which confirmed the expected m/z values for the various charge states of each adduct.

Mass Spectrometry Analyses. Two pentapeptides (PPA and PPB) with the same amino acid sequence as the A and B chain N-terminuses, respectively, of insulin were used to monitor the reaction rate of ITCs. Solutions (180 μM) of the peptides were prepared in PBS buffer at pH 7.4. Stock solutions (100 mM) of ITCs (PY-ITC, SF) were made in dimethyl sulfoxide (DMSO). For reaction, 30 μL of DMSO stock was added to 970 μL of the peptide solution, to give an initial ITC concentration of 3 mM (a 16.4 fold excess). The reaction was heated at 37 °C, and samples were injected at 1 h intervals, over 18 h, onto an LC-MS system equipped with C18 reverse phase column and electrospray detection. Ion peak areas corresponding to both starting materials and mono- and disubstituted products were monitored by selective ion monitoring (SIM) of the appropriate $[M + H]^+$ m/z value. The stability of the pentapeptides alone in PBS over 18 h was confirmed in the same way.

Cell Culture and Treatment with ITCs. Human cell lines from hepatocellular liver carcinoma (HepG2) (No. 85011430), colon adenocarcinoma (Caco-2) (No. 86010202), normal post pubertal prostate (PNT1A) (No. 95012614), and prostate adenocarcinoma (PC3) were obtained from the European Collection of Cell Culture (ECACC). The human Caucasian prostate adenocarcinoma DU145 cell line was obtained from the American Type Culture Collection (ATCC) (No. HTB-81). HepG2, Caco-2, PNT1A, PC3, and DU145 cells were routinely cultured in RPMI with 20% fetal bovine serum (FBS), DMEM (10% FBS), RPMI (10% FBS), HAMS (10% FBS), and EMEM (10% FBS) media, respectively. All human cell lines were grown to 70−80% confluence before incubation in complete media with various concentrations of ITCs for 24 h in a humidified atmosphere containing 5% CO_2 at 37 °C. ITCs were dissolved in DMSO to prepare 100 mM stock solutions, and 0.01% DMSO (final concentration) was used as control.

Cell Viability and Proliferation Assays. The effect of PY-ITC and SF on cell viability and proliferation was evaluated using a WST-1 cell proliferation kit (Roche Applied Science) and BrdU ELISA (Roche Applied Science), respectively. Cells were seeded in 96-well culture plates and allowed to adhere to the plate surface for 36 h before being exposed to various concentrations of ITCs (0−200 μM) for 24 h in six replicates. WST-1 (4-[3-(4-iodophenyl)-2-(4-nitrophenyl)-2H-5-tetrazolio]-1, 3-benzene disulfonate) reagent was then added to each well and incubated for 40 min in a humidified atmosphere (37 °C, 5% CO_2). Formazan dye produced by metabolically active cells was measured at 450 nm by microplate ELISA reader (ELx808, Ultra Microplate Reader; BIO-TEK Instruments, Inc., Winooski, VT). BrdU labeling solution (10 μL/well, final concentration 10 μM BrdU) was added to each well and incubated overnight at 37 °C. The incubation with anti-BrdU-POD was performed for 2 h at room temperature. Chemiluminescence was measured using a microplate luminometer (Luminoskan Ascent, Thermo Labsystems).

Western Blotting Analysis. PNT-1A and PC3 cells were plated in 6-well culture plates at a density of (2−4) × 10^3 cells/cm^2. After 48 hours, culture medium was removed and replaced with fresh medium to start the treatment with test compounds (0−15 μM PY-ITC; 0−25 μM SF) for 24 h. Cells were treated with vehicle (DMSO) alone in the same experimental conditions. Proteins (20 μg) were separated by 10% sodium dodecyl sulfate (SDS)-polyacrylamide gel electrophoresis and transferred to nitrocellulose membranes. The anti-p21Waf1/Cip1 (Cat. No. 2947), antiphospho-Akt (Ser473) (Cat. No. 4058), anti-Akt (pan) (Cat. No. 4685), antiphospho-p44/42 MAPK (phospho-Erk1/2) (Thr202/Tyr204) (Cat. No. 4377), and anti-p44/42 MAPK (Erk1/2) (Cat. No. 9102) antibodies were incubated at the dilutions and times recommended in the manufacturer's instructions. Membranes were processed with SuperSignal West Pico Chemiluminescent Substrate (PIERCE), visualized by Fluor s-Max Multi-Imager System (Biorad Laboratories, Inc.), and individual protein bands were quantified by the Quantity One software (Biorad Laboratories). Glyceraldehyde-3-phosphatase dehydrogenase (GAPDH) was detected as a loading control for all blots using a specific antibody (Cat.No.4300, Ambion, Inc.).

Gene Expression Analysis. PNT1A and PC3 cells were cultured for 48 h before the culture medium was removed and replaced with fresh medium containing the PI3 Kinase Inhibitor LY294002 (Cat. No. 9901, Cell Signaling Technology, Inc.) at the final concentration of 50 μM or vehicle DMSO for 1 h. Cells were subsequently treated with 10 μM PY-ITC, 10 μM SF, or vehicle DMSO, for 8 h, in triplicate. Total RNA was isolated from cells using RNeasy Mini kit (QIAGEN), and DNA digestion was performed using the RNase-Free DNase set according to the manufacturer's protocols. Gene expression profiling was performed using the Affymetrix GeneChip Human Exon 1.0 ST Array (Affymetrix, Santa Clara, CA) at the Nottingham *Arabidopsis* Stock Centre (Nottingham, U.K.) according to the Affymetrix protocols. Data were analyzed using R/Bioconductor[37] and the aroma.affymetrix package.[38] Out of a total of 36 arrays hybridized, initial analysis identified one as an array outlier and was removed before subsequent analysis. Linear probe level models were fit to RMA-background corrected and quantile normalized data to get gene-level summaries. For annotation we used the current custom CDF file available at the aroma.affymetrix Web site containing the core probesets (18 708 transcript clusters; 284 258 probesets). Subsequent statistical data analysis to identify differentially expressed genes was performed using limma.[39] Genes were identified as differentially expressed at different Benjamini and Hochberg adjusted p-values. To identify pathways that were the most overpresented in the lists of differentially expressed genes, functional analyses using the Database for Annotation, Visualization and Integrated Discovery v6.7 (DAVID; http://david.abcc.ncifcrf.gov/) was used.[40] Microarray data

generated in this study are compliant to MIAME criteria and are publicly available through ArrayExpress (E-MEXP-3640).

■ ASSOCIATED CONTENT

Supporting Information

MS insulin adducts SF. ITCs with variable side chains interact with multiple biologically relevant nucleophiles. Predicted m/z values for adducts of peptides PPA and PPB with SFN and PY-ITC, used to selectively ion monitor products, to quantify reaction rate constants. Functional analysis of genes changed by the PI3K inhibitor LY294002 in normal PNT1A cells and cancer PC3 cells. Functional analysis of genes changed by the PY-ITC in the presence of the PI3K inhibitor LY294002 in PNT1A cells and PC3 cells. This material is available free of charge via the Internet at http://pubs.acs.org.

■ AUTHOR INFORMATION

Corresponding Author

*E-mail: maria.traka@ifr.ac.uk. Phone: +44 (0)1603 255000.

Author Contributions

A.M. performed cell studies. M.H.T. performed microarray studies. P.W.N. performed chemical synthesis and kinetics. R.F.M. and M.H.T. were responsible for the inception and together with A.M. designed the study. M.H.T. took overall leadership of the study and analysis of data. The manuscript was written through contributions of all authors. All authors have given approval to the final version of the manuscript.

Notes

The authors declare no competing financial interest.

■ ACKNOWLEDGMENTS

This work was supported by funds made available from Plant Bioscience Limited (PBL) and a Biotechnology and Biological Sciences Research Council (BBSRC) Institute Strategic Programme grant to the Institute of Food Research.

■ ABBREVIATIONS USED

ITC, isothiocyanate; PY-ITC, 2-(2-pyridyl) ethyl isothiocyanate; SF, sulforaphane; CYP, cytochrome; Nrf2, nuclear factor (erythroid-derived) 2; PI3K, phosphatidylinositol-3-kinase; Keap1, Kelch-like ECH-associated protein 1; TLR, Toll-like receptor; MIF, macrophage inhibitory factor; TGF-β, transforming growth factor- beta; ARE, antioxidant response element; CDK, cyclin-dependent kinase; MAPK, mitogen-activated protein kinase

■ REFERENCES

(1) Lamy, E.; Scholtes, C.; Herz, C.; Mersch-Sundermann, V. Pharmacokinetics and pharmacodynamics of isothiocyanates. *Drug Metab. Rev.* **2011**, *43*, 387−407.

(2) Juge, N.; Mithen, R. F.; Traka, M. Molecular basis for chemoprevention by sulforaphane: a comprehensive review. *Cell. Mol. Life Sci.* **2007**, *64*, 1105−1127.

(3) Traka, M.; Gasper, A. V.; Melchini, A.; Bacon, J. R.; Needs, P. W.; Frost, V.; Chantry, A.; Jones, A. M.; Ortori, C. A.; Barrett, D. A.; Ball, R. Y.; Mills, R. D.; Mithen, R. F. Broccoli consumption interacts with GSTM1 to perturb oncogenic signalling pathways in the prostate. *PLoS One* **2008**, *3*, e2568.

(4) Traka, M. H.; Spinks, C. A.; Doleman, J. F.; Melchini, A.; Ball, R. Y.; Mills, R. D.; Mithen, R. F. The dietary isothiocyanate sulforaphane modulates gene expression and alternative gene splicing in a PTEN null preclinical murine model of prostate cancer. *Mol. Cancer* **2010**, *9*, 189.

(5) Zhang, Y. The molecular basis that unifies the metabolism, cellular uptake and chemopreventive activities of dietary isothiocyanates. *Carcinogenesis* **2012**, *33*, 2−9.

(6) Mi, L.; Di Pasqua, A. J.; Chung, F. L. Proteins as binding targets of isothiocyanates in cancer prevention. *Carcinogenesis* **2011**, *32*, 1405−1413.

(7) Hong, F.; Freeman, M. L.; Liebler, D. C. Identification of sensor cysteines in human Keap1 modified by the cancer chemopreventive agent sulforaphane. *Chem. Res. Toxicol.* **2005**, *18*, 1917−1926.

(8) Ahn, Y. H.; Hwang, Y.; Liu, H.; Wang, X. J.; Zhang, Y.; Stephenson, K. K.; Boronina, T. N.; Cole, R. N.; Dinkova-Kostova, A. T.; Talalay, P.; Cole, P. A. Electrophilic tuning of the chemoprotective natural product sulforaphane. *Proc. Natl. Acad. Sci. U.S.A.* **2010**, *107*, 9590−9595.

(9) Hu, C.; Nikolic, D.; Eggler, A. L.; Mesecar, A. D.; van Breemen, R. B. Screening for natural chemoprevention agents that modify human Keap1. *Anal. Biochem.* **2011**, *421*, 108−114.

(10) Dinkova-Kostova, A. T.; Holtzclaw, W. D.; Cole, R. N.; Itoh, K.; Wakabayashi, N.; Katoh, Y.; Yamamoto, M.; Talalay, P. Direct evidence that sulfhydryl groups of Keap1 are the sensors regulating induction of phase 2 enzymes that protect against carcinogens and oxidants. *Proc. Natl. Acad. Sci. U.S.A.* **2002**, *99*, 11908−11913.

(11) Janke, C.; Bulinski, J. C. Post-translational regulation of the microtubule cytoskeleton: mechanisms and functions. *Nat. Rev. Mol. Cell. Biol.* **2011**, *12*, 773−786.

(12) Mi, L.; Xiao, Z.; Hood, B. L.; Dakshanamurthy, S.; Wang, X.; Govind, S.; Conrads, T. P.; Veenstra, T. D.; Chung, F. L. Covalent binding to tubulin by isothiocyanates. A mechanism of cell growth arrest and apoptosis. *J. Biol. Chem.* **2008**, *283*, 22136−22146.

(13) Mi, L.; Gan, N.; Cheema, A.; Dakshanamurthy, S.; Wang, X.; Yang, D. C.; Chung, F. L. Cancer preventive isothiocyanates induce selective degradation of cellular alpha- and beta-tubulins by proteasomes. *J. Biol. Chem.* **2009**, *284*, 17039−17051.

(14) Mi, L.; Gan, N.; Chung, F. L. Aggresome-like structure induced by isothiocyanates is novel proteasome-dependent degradation machinery. *Biochem. Biophys. Res. Commun.* **2009**, *388*, 456−462.

(15) Youn, H. S.; Kim, Y. S.; Park, Z. Y.; Kim, S. Y.; Choi, N. Y.; Joung, S. M.; Seo, J. A.; Lim, K. M.; Kwak, M. K.; Hwang, D. H.; Lee, J. Y. Sulforaphane suppresses oligomerization of TLR4 in a thiol-dependent manner. *J. Immunol.* **2010**, *184*, 411−419.

(16) Healy, Z. R.; Liu, H.; Holtzclaw, W. D.; Talalay, P. Inactivation of tautomerase activity of macrophage migration inhibitory factor by sulforaphane: a potential biomarker for anti-inflammatory intervention. *Cancer Epidemiol., Biomarkers Prev.* **2011**, *20*, 1516−1523.

(17) Cross, J. V.; Rady, J. M.; Foss, F. W.; Lyons, C. E.; Macdonald, T. L.; Templeton, D. J. Nutrient isothiocyanates covalently modify and inhibit the inflammatory cytokine macrophage migration inhibitory factor (MIF). *Biochem. J.* **2009**, *423*, 315−321.

(18) Brown, K. K.; Blaikie, F. H.; Smith, R. A.; Tyndall, J. D.; Lue, H.; Bernhagen, J.; Winterbourn, C. C.; Hampton, M. B. Direct modification of the proinflammatory cytokine macrophage migration inhibitory factor by dietary isothiocyanates. *J. Biol. Chem.* **2009**, *284*, 32425−32433.

(19) Goosen, T. C.; Kent, U. M.; Brand, L.; Hollenberg, P. F. Inactivation of cytochrome P450 2B1 by benzyl isothiocyanate, a chemopreventative agent from cruciferous vegetables. *Chem. Res. Toxicol.* **2000**, *13*, 1349−1359.

(20) Moreno, R. L.; Goosen, T.; Kent, U. M.; Chung, F. L.; Hollenberg, P. F. Differential effects of naturally occurring isothiocyanates on the activities of cytochrome P450 2E1 and the mutant P450 2E1 T303A. *Arch. Biochem. Biophys.* **2001**, *391*, 99−110.

(21) Prawan, A.; Saw, C. L.; Khor, T. O.; Keum, Y. S.; Yu, S.; Hu, L.; Kong, A. N. Anti-NF-kappaB and anti-inflammatory activities of synthetic isothiocyanates: effect of chemical structures and cellular signaling. *Chem.-Biol. Interact.* **2009**, *179*, 202−211.

(22) Prawan, A.; Keum, Y. S.; Khor, T. O.; Yu, S.; Nair, S.; Li, W.; Hu, L.; Kong, A. N. Structural influence of isothiocyanates on the antioxidant response element (ARE)-mediated heme oxygenase-1 (HO-1) expression. *Pharm. Res.* **2008**, *25*, 836−844.

(23) Zhang, Y.; Kensler, T. W.; Cho, C. G.; Posner, G. H.; Talalay, P. Anticarcinogenic activities of sulforaphane and structurally related synthetic norbornyl isothiocyanates. *Proc. Natl. Acad. Sci. U.S.A.* **1994**, *91*, 3147−3150.
(24) Berglund, M.; Dalence-Guzman, M. F.; Skogvall, S.; Sterner, O. SAR studies of capsazepinoid bronchodilators 3: The thiourea part (coupling region) and the 2-(4-chlorophenyl)ethyl moiety (C-region). *Bioorg. Med. Chem.* **2008**, *16*, 2529−2540.
(25) Liang, J.; Slingerland, J. M. Multiple roles of the PI3K/PKB (Akt) pathway in cell cycle progression. *Cell Cycle* **2003**, *2*, 339−345.
(26) Melchini, A.; Costa, C.; Traka, M.; Miceli, N.; Mithen, R.; De Pasquale, R.; Trovato, A. Erucin, a new promising cancer chemopreventive agent from rocket salads, shows anti-proliferative activity on human lung carcinoma A549 cells. *Food Chem. Toxicol.* **2009**, *47*, 1430−1436.
(27) Traka, M. H.; Chambers, K. F.; Lund, E. K.; Goodlad, R. A.; Johnson, I. T.; Mithen, R. F. Involvement of KLF4 in sulforaphane- and iberin-mediated induction of p21(waf1/cip1). *Nutr. Cancer* **2009**, *61*, 137−145.
(28) Shulkla, S.; MacLennan, G. T.; Hartman, D. J.; Fu, P.; Resnick, M. I.; Gupta, S. Activation of PI3K-Akt signaling pathway promotes prostate cancer cell invasion. *Int. J. Cancer* **2007**, *121*, 1424−1432.
(29) Sarker, D.; Reid, A. H.; Yap, T. A.; de Bono, J. S. Targeting the PI3K/AKT pathway for the treatment of prostate cancer. *Clin. Cancer Res.* **2009**, *15*, 4799−4805.
(30) Bartholomeusz, C.; Gonzalez-Angulo, A. M. Targeting the PI3K signaling pathway in cancer therapy. *Expert Opin. Ther. Targets* **2012**, *16*, 121−130.
(31) Fred Hutchinson Cancer Research Center. In Vivo Effects of Sulforaphane Supplementation on Normal Human Prostate. In *ClinicalTrials.gov [Internet]*; National Library of Medicine: Bethesda, MD, 2000, cited 2012 June 21. Available from http://clinicaltrials.gov/ct2/show/NCT00946309, NLM Identifier: NCT00946309.
(32) National Cancer Institute. Chemoprevention of Prostate Cancer, HDAC Inhibition and DNA Methylation. In *ClinicalTrials.gov [Internet]*; National Library of Medicine: Bethesda, MD, 2000, cited 2012 June 21. Available from http://clinicaltrials.gov/ct2/show/NCT01265953, NLM Identifier:NCT01265953.
(33) OHSU Knight Cancer Institute. Sulforaphane in Treating Patients With Recurrent Prostate Cancer. In *ClinicalTrials.gov [Internet]*; National Library of Medicine: Bethesda, MD, 2000, cited 2012 June 21. Available from http://clinicaltrials.gov/ct2/show/NCT01228084, NLM Identifier:NCT01228084.
(34) Haristoy, X.; Angioi-Duprez, K.; Duprez, A.; Lozniewski, A. Efficacy of sulforaphane in eradicating Helicobacter pylori in human gastric xenografts implanted in nude mice. *Antimicrob. Agents Chemother.* **2003**, *47*, 3982−3984.
(35) Johansson, N. L.; Pavia, C. S.; Chiao, J. W. Growth inhibition of a spectrum of bacterial and fungal pathogens by sulforaphane, an isothiocyanate product found in broccoli and other cruciferous vegetables. *Planta Med.* **2008**, *74*, 747−750.
(36) Fahey, J. W.; Haristoy, X.; Dolan, P. M.; Kensler, T. W.; Scholtus, I.; Stephenson, K. K.; Talalay, P.; Lozniewski, A. Sulforaphane inhibits extracellular, intracellular, and antibiotic-resistant strains of Helicobacter pylori and prevents benzo[a]pyrene-induced stomach tumors. *Proc. Natl. Acad. Sci. U.S.A.* **2002**, *99*, 7610−7615.
(37) Gentleman, R. C.; Carey, V. J.; Bates, D. M.; Bolstad, B.; Dettling, M.; Dudoit, S.; Ellis, B.; Gautier, L.; Ge, Y.; Gentry, J.; Hornik, K.; Hothorn, T.; Huber, W.; Iacus, S.; Irizarry, R.; Leisch, F.; Li, C.; Maechler, M.; Rossini, A. J.; Sawitzki, G.; Smith, C.; Smyth, G.; Tierney, L.; Yang, J. Y.; Zhang, J. Bioconductor: open software development for computational biology and bioinformatics. *Genome Biol.* **2004**, *5*, R80.
(38) Bengtsson, H.; Simpson, K.; Bullard, J.; Hansen, K. *aroma.affymetrix: A Generic Framework in R for Analyzing Small to Very Large Affymetrix Data Sets in Bounded Memory*; Tech Report #745; Department of Statistics, University of California: Berkeley, CA, 2008.
(39) Smyth, G. K. Linear models and empirical bayes methods for assessing differential expression in microarray experiments. *Stat. Appl. Genet. Mol. Biol.* **2004**, *3*, Article3.
(40) Huang da, W.; Sherman, B. T.; Lempicki, R. A. Systematic and integrative analysis of large gene lists using DAVID bioinformatics resources. *Nat. Protoc.* **2009**, *4*, 44−57.